TRANSFORMATION OF ACOUSTIC EMISSION PATTERN RECOGNITION FEATURES

Mark A. Friesel

Pacific Northwest Laboratory
Operated by Battelle Memorial Institute
Battelle Boulevard
Richland, WA 99352

INTRODUCTION

Probably the most persistent general problem in acoustic emission (AE) applications is signal source identification. Past applications of pattern recognition techniques to AE have been successful, but require measurement of a parameter such as source location, load, etc., which is well-correlated with specific source types, in addition to AE signal characteristics used as the basis of the feature [1,2]. A training set comprised of a subset of the test data has also been required since good classification features and the distribution of their values are only appropriate when applied to the specific test from which they were obtained. The solution to these problems is to find robust features, or a way to predict features and feature values. Some empirical work along these lines has been done by Pacific Northwest Laboratory (PNL), operated by Battelle Memorial Institute [1,3,4]. In this paper, a transfer function between power spectral density (PSD) feature sets is established to relate the responses of two detection channels to a given source. The method may aid in identifying robust features and in predicting feature value distributions from calibration and *a priori* information.

Theoretical Development

An AE signal is captured as a transient voltage signal v(t), which includes the response e(t) of the AE sensor and electronics, hardware, or software windowing w(t), a spatial derivative of the Green's function (for dipole sources) $\partial g_{ij}(\mathbf{x},\mathbf{x_o},t)/\partial x_{k'}=g_{ij,k'}$ and a source moment $M_{jk'}(t)$ [5,6]. Given a sensor responsive to displacement in the i direction,

$$v(t) = w(t)[e(t)*g_{ij,k'}*M_{jk'}] \qquad (1)$$

where * denotes convolution. Manipulation is simpler in the Fourier domain where

$$V(\omega) = W(\omega)*[E(\omega)G_{ij,k'}(\omega)M_{jk'}(\omega)]. \qquad (2)$$

Although the sensor response and windowing functions may affect the signal significantly (the analysis in the appendix of Chang and Sachse [7], is incorrect), these effects are considered determinable and the factors are dropped.

Review of Progress in Quantitative Nondestructive Evaluation, Vol. 9
Edited by D.O. Thompson and D.E. Chimenti
Plenum Press, New York, 1990

The displacement vector due to a p-wave mode in the far-field, with separable $M_{pq'} = m_{pq'}s(t)$ and isotropic time dependance, has components

$$u_n = (4\pi r c_1^2)^{-1} \mu_n \mu_p \mu_q m_{pq'} \dot{s}(t - r/c_1) \qquad (3a)$$

which transforms to

$$U_n(\omega) = (\text{spatial terms}) i\omega \exp(i\omega r/c_1) S(\omega) \qquad (3b)$$

giving a PSD function in an arbitrary direction $\mathbf{u} \cdot \boldsymbol{\mu}$ of

$$P(\omega) = (\text{spatial terms}) \omega^2 S^2(\omega) \qquad (4)$$

In Eq. (3) c_1 is the longitudinal wavespeed, μ_j are direction cosines, r is the source/sensor distance, ω is the frequency, and $\dot{}$ denotes differentiation. The PSD obtained through some channel A at one location can, therefore, be related to that of a different channel B at a second location by

$$P_B(\omega) = \frac{(\quad)_B}{(\quad)_A} P_A(\omega) = H P_A(\omega) \qquad (5)$$

where the brackets ( ) enclose spatial terms.

This form seems to generally hold for signals dominated by a specific wavemode. The frequency-dependent source terms are seen to cancel in H; and for this case, H is frequency independent. After normalization, the distribution of feature values for a PSD feature are therefore the same on both channels. Rayleigh wavemodes, which dominate in the far-field of thick sections, are also representable in the above form and can be similarly related [5]. Investigation of the transfer function for these modes may be of benefit in AE testing of thick structures. A similar relationship may be found for flexure in thin plates, where for a simple force input with time dependence $\partial s(t)/\partial t$, the vertical displacement at a distance r is given by [8]:

$$u(r,t) = s(t) * (a/t) \sin[r^2/4bt] \qquad (6)$$

where b depends on material constants. The transfer function in this case is both r and ω dependent, but again does not contain source effects.

Most AE signals are comprised of multiple modes or near-field responses. These introduce terms in the transfer function with different frequency dependence depending on whether the derivative of the source moment is involved or not, and on the difference in arrival times of the various modes. Spatial effects cannot usually, therefore, be removed through normalization. As an example, the transfer function in the far-field due to arrival of the p- and s-waves can be written:

$$H(\omega) = \frac{a_B + b_B \cos[\omega r_B (s_2 - s_1)]}{a_A + b_A \cos[\omega r_A (s_2 - s_1)]} \qquad (7)$$

In most AE applications, the range of frequencies is less than about 1 MHz. With reasonable r values, $\omega r/s_2$ varies over a substantial part of a cycle or more, and $H(\omega)$ is strongly affected by frequency and changes in r. Figure 1 illustrates how $H(\omega)$ changes with frequency and sensor placement for r_A = 5 cm and various values of r_B over a frequency range of 0 to 1 MHz. The transfer function can be calculated if the flaw size and location is known, say for instance from UT examination. If reference data is available, this method may offer some advantage over

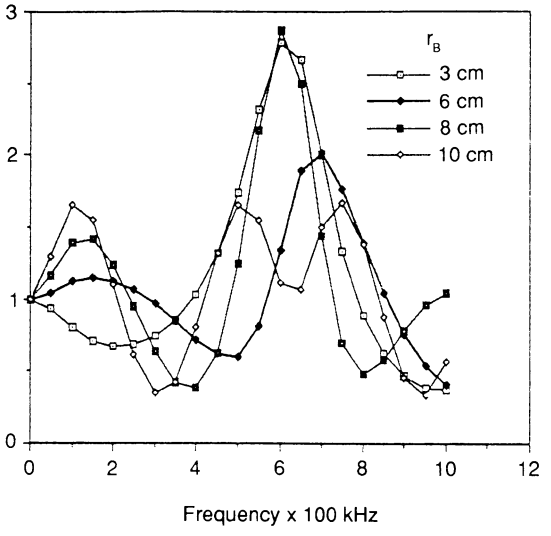

Fig. 1. Change in $H(\omega)$ with frequency and channel B sensor distance for r_A = 5 cm.

direct calculation in the manner of Eq. (1), particularly if the source function or instrument response function is unknown.

Calibration is *a priori* information which may be useful for feature prediction. Again ignoring surface waves, the transfer function for a point force may be derived as above using the appropriate undifferentiated Green's function, and a simple force rather than the moment [5]. The form of $H(\omega)$ for p- and s-waves is the same as that of Eq. (7), but the value of the constants will differ and $H(\omega)$ again does not appear to be normalizable. If the source-sensor distance is the same for calibration and the AE source, then the spectra of the calibration and AE vary in a similar fashion, although with different changes in magnitude. This similarity may be sufficient to predict usable pattern recognition features, particularly if noise sources show contrasting frequency dependence due, for example, to a different source location.

Experimental

A test performed at PNL during work sponsored by DARPA and the NADC [1] may be used for illustration. Acoustic emissions from crack growth and fretting were obtained while cyclically loading a thin, jointed aluminum plate. The experiment and equipment are described in detail elsewhere [1], hence only a cursory description will be given here. A 0.75 inch hole was milled two inches from one end of a 26 x 4 x 0.15 inch thick plate of 7075-T651 aluminum. A pin through the hole connected the plate to an assembly in such a manner as to allow the joint to rotate during sinusoidal cyclic loading. Four custom-built AE sensors, labeled A, B, P, and Q, were mounted as shown in Fig. 2. The sensors were made from 1/8 inch diameter PZT-5 bonded to a 1/2 inch diameter thin ceramic disk. With the initial 20 dB amplification stage, the sensors had a passband of roughly 200 to 750 kHz. During Phase 1 of the test, fretting emissions caused by rubbing between the pin and the joint were collected. The joint hole was then notched, and a short fatigue crack started at the notch tip. During Phase 2, AE from the growing crack were collected as well as fretting noise. The instrument was constructed to allow signals to be recorded through two channels simultaneously.

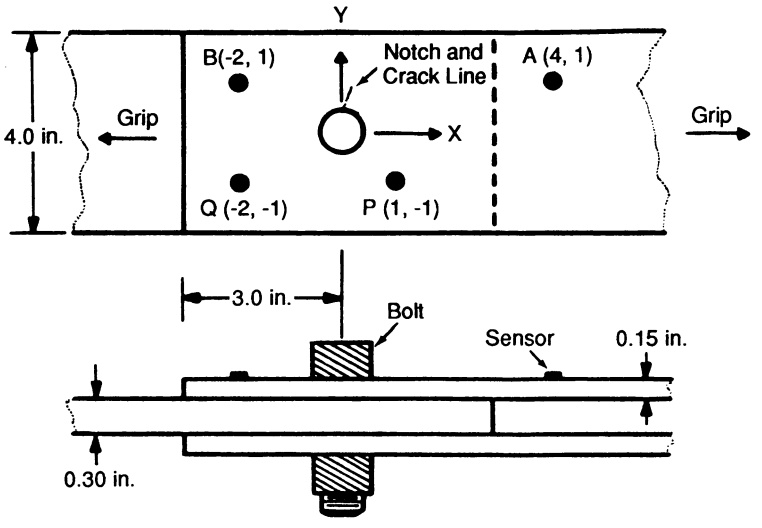

Fig. 2. Plate assembly with sensor positions

Calibration signals were collected from various locations by breaking 0.2 millimeter diameter H hardness pencil leads, using a plastic ball which fit over the point of a mechanical pencil. A set of three signals was collected from each location and specimen condition to allow some averaging capability. The ~70 dB total amplification used during the test was enough to cause the calibration signals to saturate the AE instrument, even with the small diameter leads used, therefore a 20 dB amplifier was removed from the circuit during calibration. Although the amplifier was broadband and fairly flat, some effect on signal feature values can be expected. Signals from each set were found to be quite similar in general, but substantial differences were observed between sets which probably reflected the changes in source location, load on the specimen, and the effect of the crack on signal propagation. Three sets of calibration were examined, all originating at the intersection of the line joining sensors A and B and the line through the center of the joint and the notch tip. Set 1 signals originated from the unloaded plate on the side opposite the sensors. Set 2 signals were from the same side as the sensors with the plate at minimum load, while Set 3 was obtained under the same conditions as set 2, but with the notch and a short crack present.

Figure 3 shows averaged, normalized power spectra from each of the three calibration sets, along with typical normalized spectra from AE obtained during the test, as recorded through Channel A. Fretting is labeled T3 or T5 in reference to the storage tape used for Phase 1 or Phase 2 fretting signals respectively. In Phase 2, fretting and crack growth were identified on the basis of the location of the AE events on the load cycle, with cracking assumed to originate near maximum load at load position 25, as seen in Fig. 4.

Transfer functions to convert Channel A to Channel B feature values were derived from signal pairs and averaged for each calibration set and each AE category. Crack growth and T5 fretting transfer functions are fairly similar as seen in Fig. 5, despite fretting arising from somewhat scattered locations around the pin hole rather than at the crack tip, as evidenced by rubbing residue. Set 2 and Set 3 calibration transfer functions have a fairly strong resemblance to those of Phase 2 AE but

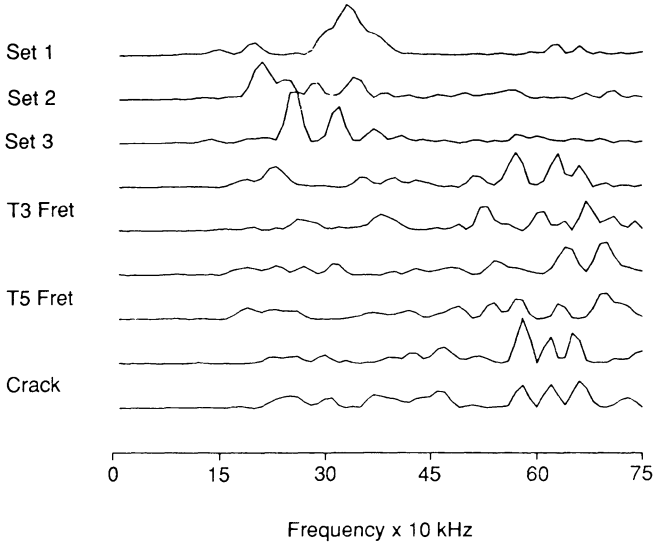

Fig. 3. Averages of normalized power spectra of three pencil lead calibration sets and representative AE data

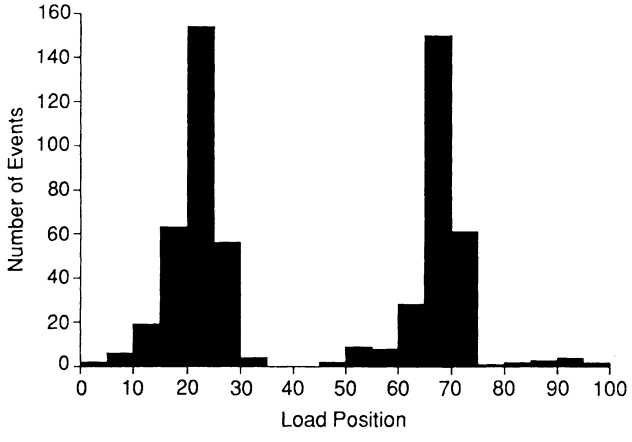

Fig. 4. Load positions of Phase II AE events

show an apparent frequency shift in some of the outstanding characteristics.

The pattern recognition procedure consisted of weighting the individual features according to their ability to separate crack growth signals from combined T3 and T5 fretting events. The feature set used was composed of the power spectra averaged over 10 kHz intervals in the passband. Autocorrelation features were initially examined as well with comparable results. Fisher and variance feature weighting were both employed and found to produce comparable classifier performance. The features were sequentially used on the basis of these weights to train the classifier, and the classifier performance was examined as a function of the number of features used. The classifier was a bi-linear least squares linear regression of the form $P_k = \Sigma a_{ik} x_i$, where x_i are values of the i features and a_{ik} are classification weights computed for each class k, so that the output P_k is 1 if the signal belongs to class k and -1

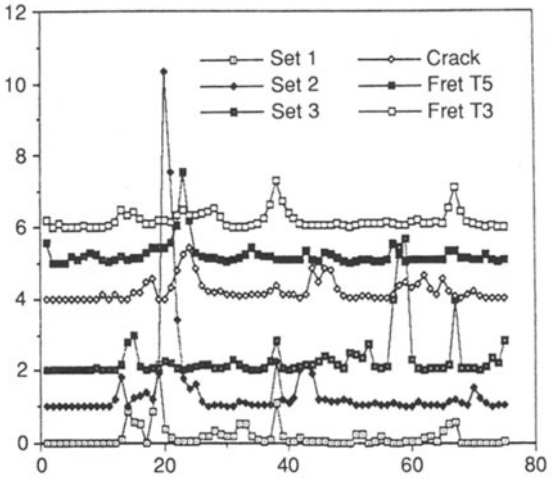

Fig. 5. Transfer functions from calibration and AE data sets

otherwise. In a bi-linear regression, the weights for class 2 are the opposite of those for class 1, and when an unclassified feature vector is analyzed, it is placed in the class whose P_k value is highest. Results using a channel A trained classifier on various data sets are shown in Fig. 6. Channel A data produces the best performance, correct fretting exceeding 90% for all but the two and three feature classifiers, while performance for crack signal classification increases to above 80% with four features and above 90% for seven features. As a control set, Channel B is also classified using the Channel A regression weights. In this case, crack identification is good, but fretting performance is poor and tends to become worse when more features are used. It is noteworthy that use of more features does not necessarily improve overall performance since the a_{ik} are recalculated whenever a new feature is added. With well-transformed data, the performance should be good using the channel A classifier. From Fig. 6, it is evident that good overall results are not attained. Channel B data transformed by the set 2 transfer function does best overall, but classification performance is still unacceptably low.

In Fig. 7, the distribution of feature values of one of the best classification features is shown. The top three plots are the distributions of feature 20 values for the two fretting sets and the crack growth data. The middle three plots are the distributions from the Channel B data, and the lower three are distributions of Channel B data transformed by the set 2 transfer function. Qualitatively, the transformation works as desired, particularly on Phase 2 AE data. Channel B distributions are lower valued than those of Channel A, and the transformation increases the values close to the desired amount. The crack feature values are low valued, and many of the Channel B crack features values are zero or differ from zero by an amount less than the 0.001 Volt resolution of the instrument. These zero values are unaffected by any finite transformation, but in this case the effect does not appear to be significant. The low crack feature values are assumed to be the principle cause of good results attained in two specific cases involving the autocorrelation function utilizing a time domain convolution [1], instances where conditions of high error tolerance were present in the classification scheme. In general, the transformation is

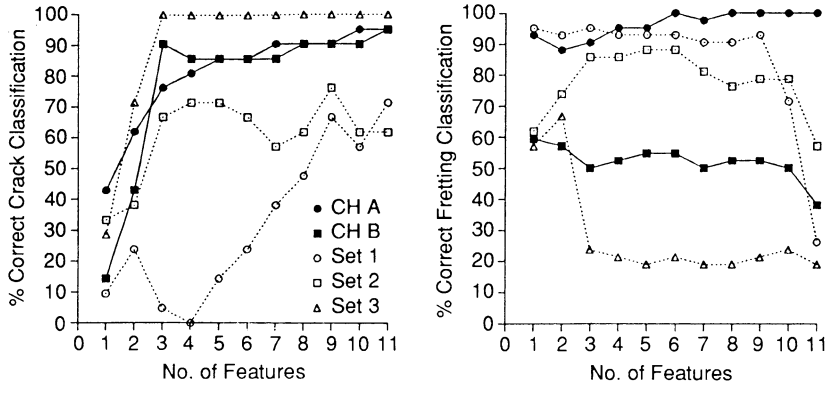

Fig. 6. Performance results for the channel A-trained classifier

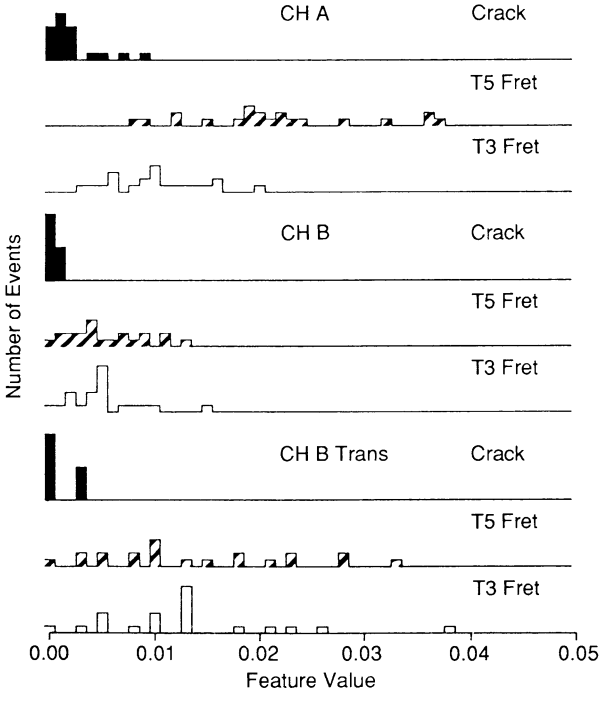

Fig. 7. PSD feature 20 value distribution

correct in direction for most features, but is numerically incorrect. Accuracy in the transformation is apparently further impeded by the instrument resolution, and also by a disparity in the factor required to correctly scale the various data sets. In some cases, a transformation which underscales crack values will overscale one of the fretting sets, although this should be expected because of the differences in plate loading when the events occur, and in differences in source location.

Discussion

Because the test was planned and performed before a transformation procedure was known to be necessary, the qualitatively correct results found for many of the features are encouraging. Obviously, the conditions deviated from the ideal in a number of ways, and questions concerning the effects of removal of the amplifier stage for calibration, zeroes in the feature value distributions, size of the transducer elements and facing plate, and the assumed similarity of calibration and crack growth transfer functions, should be addressed. In the author's opinion, the use of classifiers which rely directly on features of multiple data types are not ideal when only a single source type is of interest. In the context of the present approach to feature prediction and the above test results, a difficulty arises because the locations of the crack growth and fretting sources were not the same. A distance-dependent transfer function which accurately transformed crack signals could not be expected to maintain accuracy for sources originating elsewhere. This concern becomes more marked if the distribution of principle feature values depends more strongly on geometry than source type.

REFERENCES

1. P. H. Hutton, M. A. Friesel, L. J. Graham, R. K. Elsley, Develop In-Flight Acoustic Emission Monitoring of Aircraft to Detect Fatigue Crack Growth, NADC-81087-60, Battelle, Pacific Northwest Laboratories, Richland, Washington (1985). There is an error in App. A in the expression for the coefficients a_k of the polynomial spline function, where A_k and A_z should replace a_k and a_z on the right-hand side.
2. P. G. Bentley and M. J. Beasley, J. Acous. Emission 2(7), pp. 59-79 (1988).
3. M. A. Friesel, NDT Int'l., 19(3), June, pp. 203-206 (1986).
4. M. A. Friesel, Mat'ls Ev., 47(7), July, pp. 842-848 (1989).
5. K. Aki and Richards, P. G., Quantitative Seismology, Vol. 1, (W. H. Freeman & Co., New York, 1980).
6. N. N. Hsu and F. R. Breckenridge, Mat'ls. Eval., 39, Jan., pp. 60-68 (1981).
7. C. Chang and W. Sachse, J. Acoust. Soc. Am., 79(5), pp. 1307-1316 (1986).
8. K. F. Graff, Wave Motion In Elastic Solids, (Ohio State University Press, 1975).